Phys Chem Minerals (1985) 12:333–341

PHYSICS AND CHEMISTRY OF MINERALS
© Springer-Verlag 1985

Modulated Structures in Calcian Dolomite: A Study by Electron Microscopy

G. Van Tendeloo[1], H.R. Wenk[2] and R. Gronsky[3]

[1] Laboratory for Solid State Physics, University of Antwerp (RUCA), Groenenborgerlaan 171, 2020 Antwerp, Belgium
[2] Department of Geology and Geophysics, University of California, Berkeley, CA 94720, USA
[3] National Center for Electron Microscopy, Lawrence Berkeley Laboratory, University of California, Berkeley, CA 94720, USA

Abstract. Calcian dolomite from the Devonian Lost Burro formation has been investigated with electron microscopy techniques. Electron diffraction shows evidence for "c" and "d" type reflections which may occur independently and are indicative of ordered superstructures. High resolution electron microscopy combined with selected area optical diffraction is the basis for models to explain the superstructures in calcian dolomite. It is proposed that "c" reflections are due to ordered substitution of Mg by Ca in basal cation layers. "d" reflections result when the rhombohedral stacking of basal layers is interrupted by intercalation of additional Ca layers. During electron irradiation at 1 MeV the Mg–Ca distribution becomes disordered and the crystal structure attains calcite symmetry. The arrangement of CO_3 groups remains ordered.

1. Introduction

Rhombohedral carbonates often occur as limited solid solutions. Of particular importance is the series $CaCO_3$ (Calcite, $R\bar{3}c$) – $Ca_{0.5}Mg_{0.5}CO_3$ (dolomite, $R\bar{3}$) with intermediate members of magnesian calcite and calcian dolomite. Such non-stoichiometric carbonates are especially common in sedimentary (low temperature) rocks and are characterized by a modulated microstructure when observed with the transmission electron microscope (Reeder and Wenk 1979; Reeder 1981). The modulations have been associated with submicroscopic compositional variations in these non-stoichiometric compounds (Reeder 1981) and with distortions due to defects in the anion distribution (Gunderson and Wenk 1981) because they also occur in some pure calcites. It is possible that anion defects and deviations from stoichiometry are related (see discussion by Wenk et al. 1983). Modulations parallel to $\{10\bar{1}4\} = r$ seem to originate during special conditions of replacement growth where a secondary carbonate replaces a primary carbonate by a dissolution-reprecipitation mechanism across a thin film of aqueous solution. It has been very difficult to characterize the modulated structure by contrast experiments because the structure is strictly coherent, the wavelength (~ 10 nm) is too small to permit direct chemical analyses, and in samples studied so far, it has not been sufficiently ordered to distinguish domains with different ordering patterns.

In this paper we report observations on an unusually ordered calcian dolomite of an overall composition, $Ca_{0.54}Mg_{0.46}CO_3$, from the Devonian Lost Burro Formation in Western California, where dolomite replaces micritic limestone during late diagnetic-deep burial conditions (Zenger 1983). A preliminary TEM study (Wenk and Zenger 1983) described periodic basal faults in domains extending parallel to $\{10\bar{1}4\}$ which were interpreted as layers of additional Ca intercalated in the dolomite structure.

2. Carbonate Structures and Unit Cells

The structure of rhombohedral carbonates can be viewed as a rhombohedrally distorted NaCl structure with CO_3 groups substituting for Cl and cations (such as Ca and Mg) substituting for Na. This structure contains alternating layers of hexagonally arranged cations and CO_3 groups (Fig. 1a). In one layer all CO_3 groups point in the same direction, but in the next adjacent layer they point in the opposite direction (Fig. 1b). In *calcite*, $CaCO_3$ cations are arranged in a three-layer periodicity with an ABC stacking; but anion groups, due to their different orientation, have a six-layer periodicity which determines the c lattice parameter ($c = 1.706$ nm) (Table 1). The space group of calcite is $R\bar{3}c$ and can be described in a rhombohedral or a non-primitive hexagonal unit cell. The hexagonal unit cell ($a = 5$ nm, $c = 17$ nm) is used throughout this paper and all indices refer to it. We use three symbol Lave indices, hkl, whenever diffraction is emphasized and four symbol Miller-Bravais indices, $hkil$, $i = -(h+k)$, whenever morphologic planes and directions are discussed. In a hexagonally indexed diffraction pattern, reflections of the type $-h+k+l \neq 3n$ are extinct due to rhombohedral symmetry. Reflections that are present in calcite are termed "a" reflections. Tables 1 and 2 summarize the lattice geometry of rhombohedral carbonates and related structures and define reflection types.

In $NaNO_3$, which is isostructural with calcite, NO_3 groups are disordered above 273° C, pointing at random in one direction or its opposite (Paul and Pryor 1971). This increases the symmetry to $R\bar{3}m$. All "a_2" reflections are extinct, and the unit cell is effectively shortened along z by one half.

Ordering the cations in *dolomite*, $Ca_{0.5}Mg_{0.5}CO_3$, on alternate layers reduces the symmetry to $R\bar{3}$. Therefore "b" reflections which were extinct in calcite are present in dolomite.

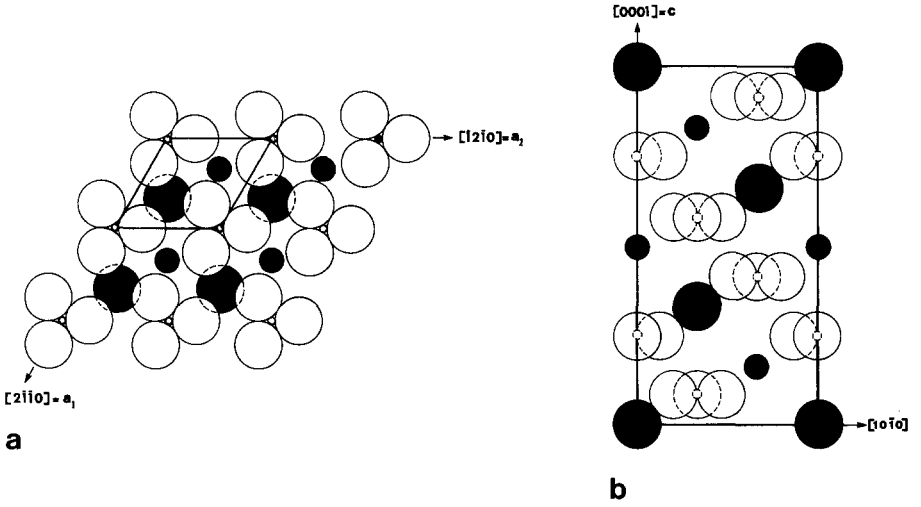

Fig. 1 a, b. Structure of dolomite $(Ca, Mg)CO_3$.
a Viewed along [0001];
b viewed along $[\bar{1}2\bar{1}0]$. Unit cells in both projections are indicated. Large open circles are oxygen atoms; small open circles are carbon atoms. Large black dots represent Ca atoms, whereas small black dots are Mg atoms

Table 1

Structure	Calcite with disordered CO_3 groups	Calcite	Dolomite	"c" dolomite	"d" dolomite
Space group	$R\bar{3}m$	$R\bar{3}c$	$R\bar{3}$	$P2/m$	$P\bar{6}m2$
Bravais Lattice	rhombohedral	rhombohedral	rhombohedral	monoclinic	hexagonal
Conditions Limiting Reflections	$hkl: -h+k+l=3n$ $l=2n$ (relative to calcite cell)	$hkl: -h+k+l=3n$ $hhl: l=2n$	$hkl: -h+k+l=3n$	–	
Type of Reflections	a_1	$a=a_1+a_2$	a, b	a, b, c	a, b, d

Table 2. Types of reflections (with reference to the calcite unit cell)

Type of reflection	Conditions for presence of reflections	Structural reason
a_1	hkl, l=even, $-h+k+l=3n$	due to the basic structure
a_2	hkl, l=odd, $-h+k+l=3n$	due to anion orientation in calcite and anion orientation plus alternating cations in dolomite
b	$hhl: l$=odd	due to cation order in dolomite
c	midway between reflections along a_1 (e.g., $h-{}^1/_2\,hl$	due to cation (or anion) ordering within a basal layer which has no 3-fold axis
d	$hkl: -h+k+l\neq 3n$	due to periodic stacking of basal cation (or anion) layers which is not rhombohedral

3. Conventional Electron Microscopy

TEM specimens were prepared by ion beam thinning (argon ions, accelerated to 5 kV with a beam current of 10 mA) of selected areas of petrographic thin sections. They were first studied with a JEM 100 C electron microsope. In Lost Burro dolomite, additional reflections to those described above appear in the diffraction patterns. Consider Figure 2a with strong reflections 110, $\bar{2}10$ and $1\bar{2}0$ which are equivalent because of rhombohedral symmetry. Between *one* of those reflections ($\bar{1}20$) and the origin there is a weak spot which destroys the hexagonal symmetry of the diffraction pattern and which cannot be indexed with the dolomite unit cell. These reflections are repeated by translation in the whole reciprocal lattice and have been termed "c" type reflections by Reeder and Wenk (1979). They are frequently observed in carbonates with a modulated microstructure. As Reeder (1981) documented, they are sometimes sharp, often diffuse and streaked parallel to a_1. Other crystals display satellites about "a" and "b" reflections (Wenk and Zenger 1983). These "d" reflections occur at one third the spacing between "a" reflections along the c^* axis and therefore effectively violate the extinctions due to the rhombohedral symmetry. They are generally fairly sharp, but often there is accompanying diffuse streaking approximately parallel to c^*. Typical diffraction patterns are shown in Figure 2, together with their schematic representations.

With conventional dark field techniques, it is possible to identify regions in the crystal which display "c" and "d" type superstructure reflections. Micrographs in Figure 3 illustrate that both occur in elongated domains, extending parallel to $\{10\bar{1}4\}=r$, i.e., parallel to the modulated structure. These domains comprise about 25% of the total volume. The elongation of the satellites along c^* is not so much related to the shape of the "c" or "d" domains but is due to the internal structure in these domains.

The domains in Lost Burro dolomite are only a few tens of nanometers wide. Even with a 5 nm beam in a STEM we could not document any significant changes in chemical composition between regions that display superstructure reflections and those that do not. This may indicate that the composition is constant, but more likely it is due to averaging effects at the high tilt angles required.

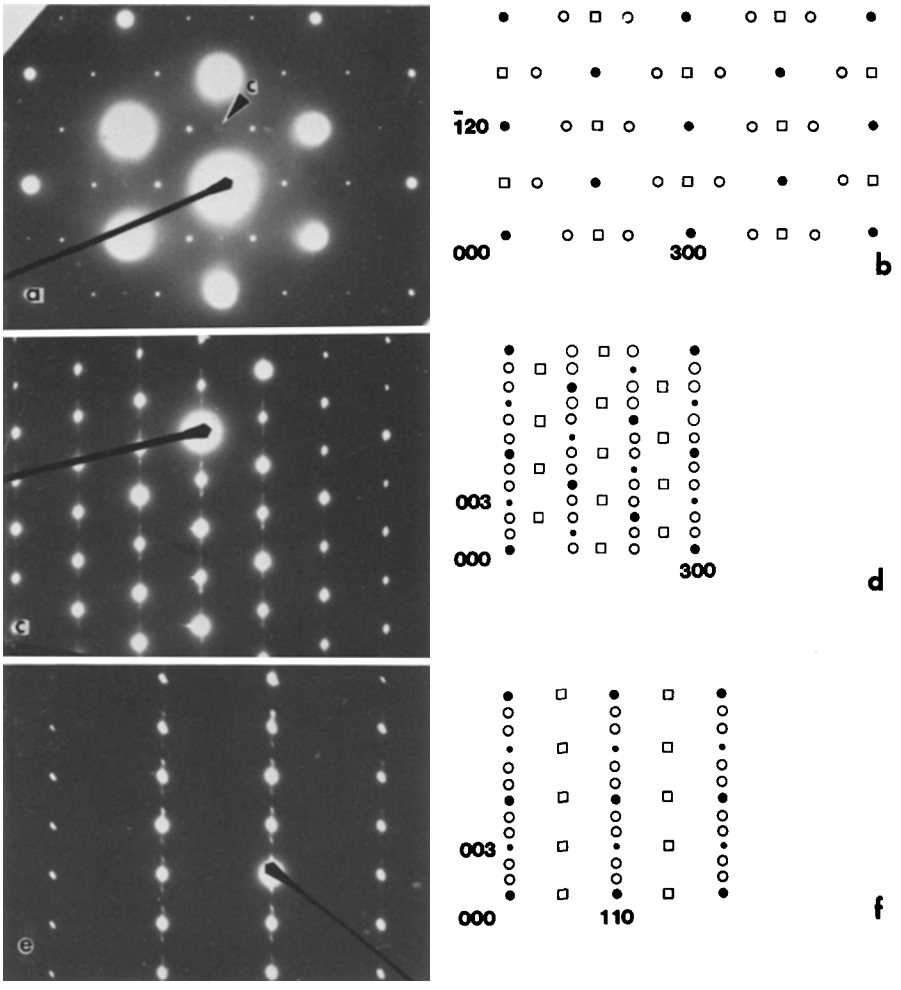

Fig. 2a–f. Diffraction patterns of Lost Burro dolomite (**a**, **c**, **e**) and schematic representations of reflection types (**b**, **d**, **f**). • "a_1", • "a_2", □ "c", ○ "d". Note that no "c" reflections appear in (c, e)

EDX analyses of the Ca/Mg ratio agree closely with microprobe analyses of the bulk crystal ($Ca_{0.54}Mg_{0.46}CO_3$).

High Resolution Observations

Conventional two-beam micrographs provide some information about microstructures in these samples. However, due to their complexities, it became desirable to use high resolution techniques to investigate local structural variations. Microscopes employed were a JEM 200 CX with top-entry stage and, for selected experiments, the JEOL JEM ARM 1000. Micrographs in Figures 4 and 5 are viewed along $a_3=[11\bar{2}0]$ (Fig. 2c), which is a direction in the carbonate structure in which only equivalent atoms are lined up parallel to the electron beam (Fig. 1), and the projection contains therefore a maximum amount of information that can be interpreted relatively easily. A typical high resolution, low magnification image is shown in Figure 4a, and the corresponding diffraction pattern is shown as an inset. The image reveals narrow strips (less than 10 nm wide) corresponding to the "d" domains. The changes in background contrast in the "d" domains as well as in the matrix indicate a great deal of distortion and strain. The "d" domains are approximately parallel to $\{10\bar{1}4\}=r$ (the trace indicated in Figure 4a belongs to a system which is not viewed edge-on and therefore there is no corresponding spot in the diffraction pattern) and within the domains faulting along (0001) can be discerned. Close to the edge of the foil, bright speckles, 1 to 5 nm large, are visible (indicated by arrows); they are most probably defects generated during the preparation of the specimen (ion beam bombardment). The amorphous edge (E) about 5 nm wide is also due to this preparation technique and increases during observation because of contamination. It is remarkable that close to the edge no "d" domains are observed; the reason for this will be discussed in more detail in a later section. However, the finding is related to the nature of these domains as well as to the small thickness of the foil near the edge (<10 nm).

It becomes obvious upon inspection of more highly enlarged portions of these micrographs that "d"-domains have a different structure from the host dolomite. Figure 4b reveals a "d" domain in between two regions of perfect dolomite. In the unfaulted regions (top right and lower left sectors) a two-layer rhombohedral unit cell (black) can be recognized. It consists of a layer of intense bright dots alternating with less intense and more diffuse dots along the c-axis. For comparable microscope conditions at Scherzer focus, O'Keefe and Barber (1984) calculated the expected images and interpreted the white dots to represent columns of Ca (bright dots) and Mg (less intense dots) in layers spaced 1.6 nm/6=2.7 nm apart. In the "d" domains, however, we recognize a hexagonal unit cell (white) consisting of a three layer repeat. The defects along c in

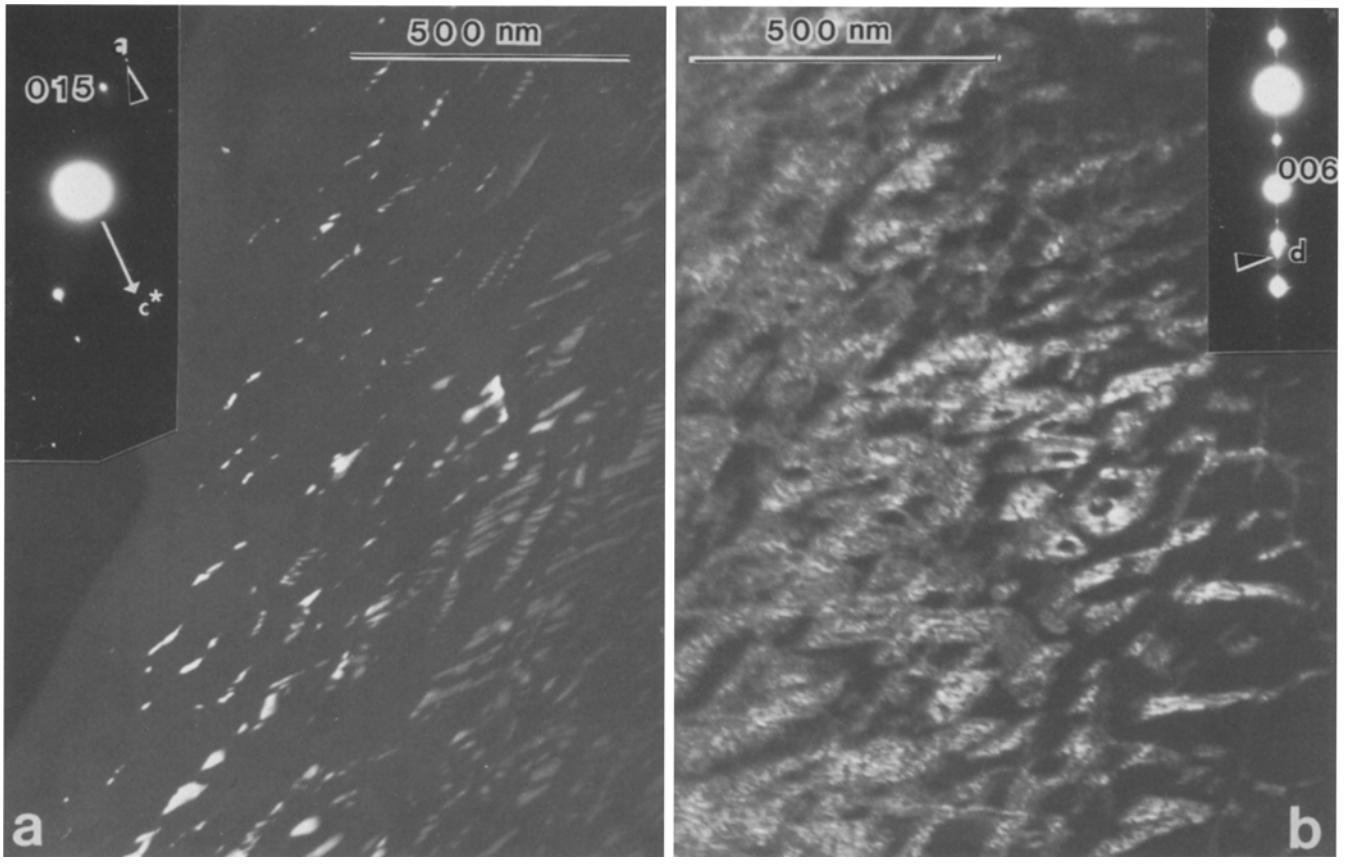

Fig. 3a, b. Dark-field images illustrating the presence of elongated domains in light contrast. **a** "c" domains; **b** "d" domains. Arrows point to operating reflections

these domains – (0001) = c is horizontal in Figure 4b – are due to narrow rhombohedral (dolomite-type) strips. Looking at the image at a glancing angle along the directions indicated R and H, we see that there are well defined boundaries between the rhombohedral dolomite (looking along R) and the "d" domains (looking along H), although the boundaries are not strictly along a low index crystallographic orientation. In thicker areas it is observed that most boundaries are also inclined with respect to the electron beam, and they are therefore not sharp.

The image contrast of the rhombohedral structure changes quite drastically but continuously, even for the same thickness and same focus. This is most probably due to a change in the local crystallographic orientation produced by the strain observed in the conventional images as well as in the low magnification HREM image (Fig. 4a).

More information about local structural heterogeneities can be obtained from optical microdiffraction using the HREM images as objects for the incident laser beam. The advantage of this technique is that one is able to produce diffraction patterns from areas as small as a few nanometers (Sinclair et al. 1976; Tanji and Hashimoto 1978; Van Tendeloo and Van Landuyt 1983). The rhombohedral areas produce a typical ($h0l$) dolomite diffraction pattern (Fig. 4c). It was found that changes in the area selected within a structural domain cause slight changes in intensity of the reflections, presumably produced by local orientation differences explaining the variation in the HREM image contrast. Selecting in the aperture only the narrow "d" domains produces a primitive hexagonal rather than a rhombohedral diffraction pattern (Fig. 4d) with no extinctions due to rhombohedral symmetry and all reflections of comparable intensity. In this pattern no streaking is observed, since a perfect hexagonal domain was selected to produce this ($h0l$) diffraction pattern. The observed streaking in the electron diffraction patterns is produced by a convolution of the effects of nonperiodic defects along (0001) = c, and the shape of "d" domains which are elongated along $\{10\bar{1}4\} = r$. In some areas, due to frequent faulting, the satellites can be hardly recognized, and an almost continuous streak along c^* is observed.

In some specimens "c"-type ordering reflections are observed; sometimes they occur together with "d" reflections, but quite commonly they are observed alone, again in domains that show a distinctly different structure at low magnification (Fig. 5a). Enlargement of portions of high resolution micrographs illustrate a doubling of the a unit cell dimension (Fig. 5b). The optical diffraction from the "c" domains (inset to Fig. 5b) confirms that no primitive hexagonal structure is involved within these regions (absence of "d" type reflections). The doubling of the periodicity along a is seen in the high resolution micrographs, but "c"-domains appear to be less regular than "d" domains, and their interfaces are not well defined.

5. Interpretation of Modulated Structures

Coherent superstructures with different symmetries are well known in ordered non-stoichiometric alloys (e.g., Van Ten-

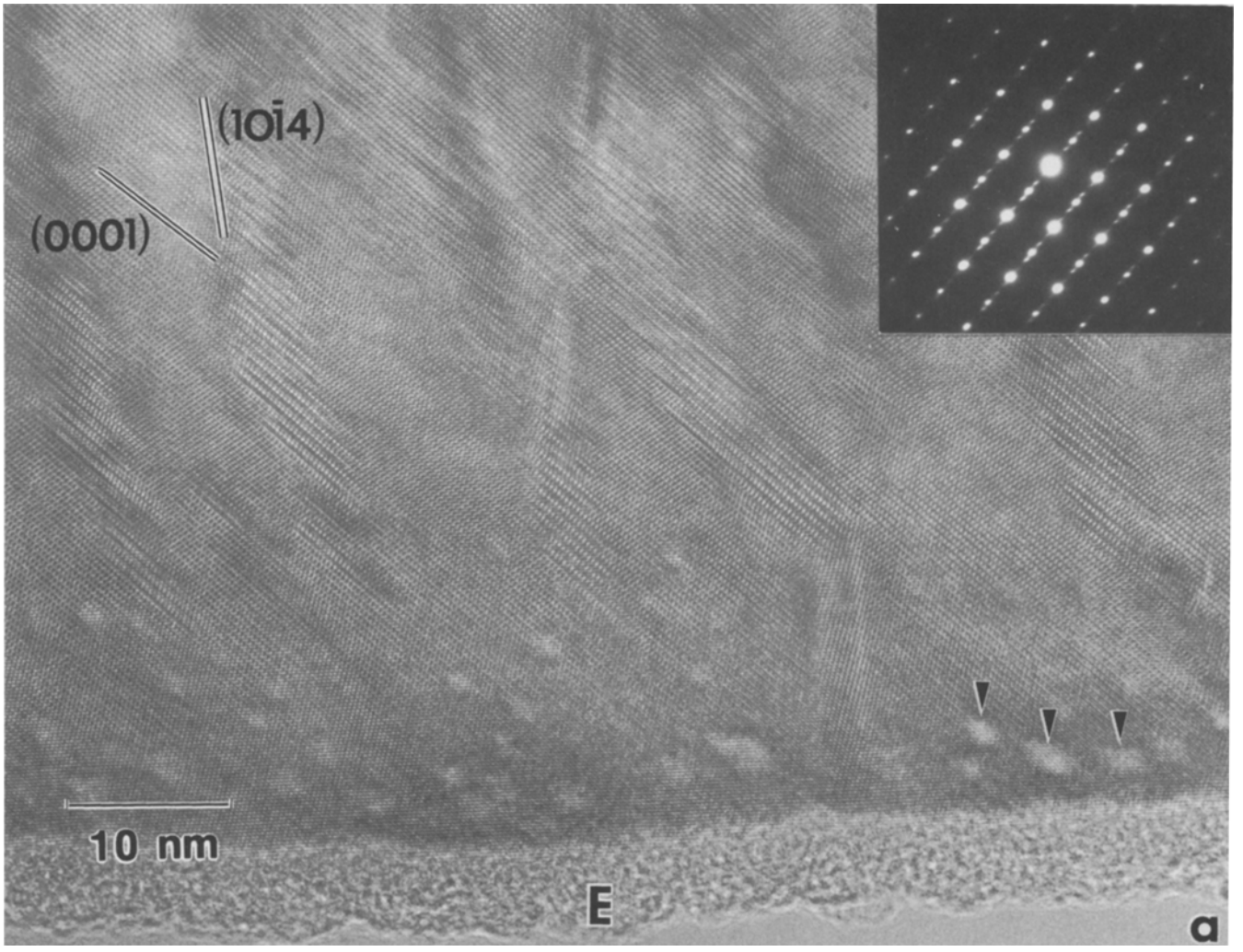

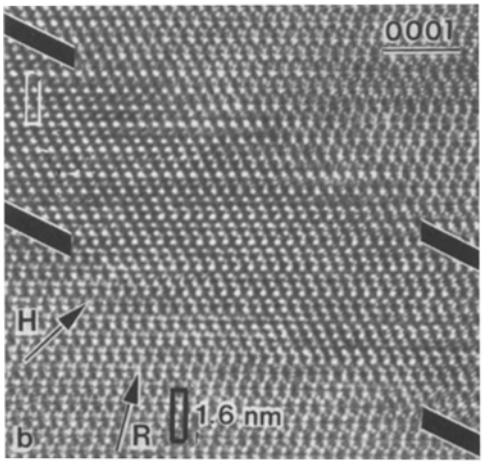

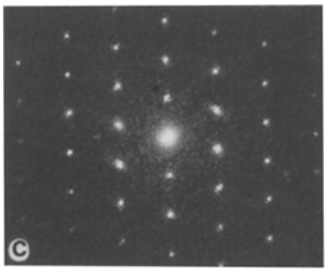

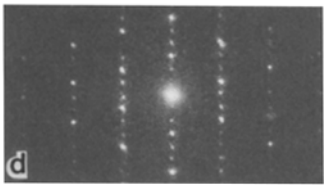

Fig. 4. a Low magnification, high resolution image along [11$\bar{2}$0] showing "d" domains aligned parallel to (10$\bar{1}$4)=*r*. Inside these domains planar defects parallel to (0001) are apparent. **b** High magnification image of "d" domain (top left to bottom right) with adjacent ideal dolomite. H and R are directions along which it is most easy to recognize the primitive hexagonal and rhombohedral stacking, respectively. Unit cells are indicated. Note that orientation of (a) and (b) are different. **c** and **d** Optical diffraction patterns of ideal dolomite region (c) and "d" domain (d) in same orientation as (b)

deloo and Amelinckx 1981; Van Tendeloo et al. 1974; Schryvers et al. 1983). In fact, many of the diffraction patterns of f.c.c.-based alloys resemble closely those of Lost Burro dolomite where cations are also arranged in a distorted, pseudo-cubic, face-centered pattern. In our interpretation we emphasize this analogy and are mainly concerned about cation ordering, although anion defects may also be present in these sedimentary carbonates (Gunderson and Wenk 1981; Wenk et al. 1983).

We distinguish two types of superstructures. The first is presumably related to stacking of basal cation layers along *c* and gives rise to "d" type satellite reflections. Such a structure was originally suggested for non-stoichiometric calcian dolomite by Goldsmith and Graf (1958) and first observed by Wenk and Zenger (1983). A second is thought to be due to ordering of cations within the basal plane and is expressed in "c" reflections.

The easiest way to interrupt the rhombohedral stacking

$$Ca^1-Mg^1-Ca^2-Mg^2-Ca^3-Mg^3-Ca^1\ldots$$

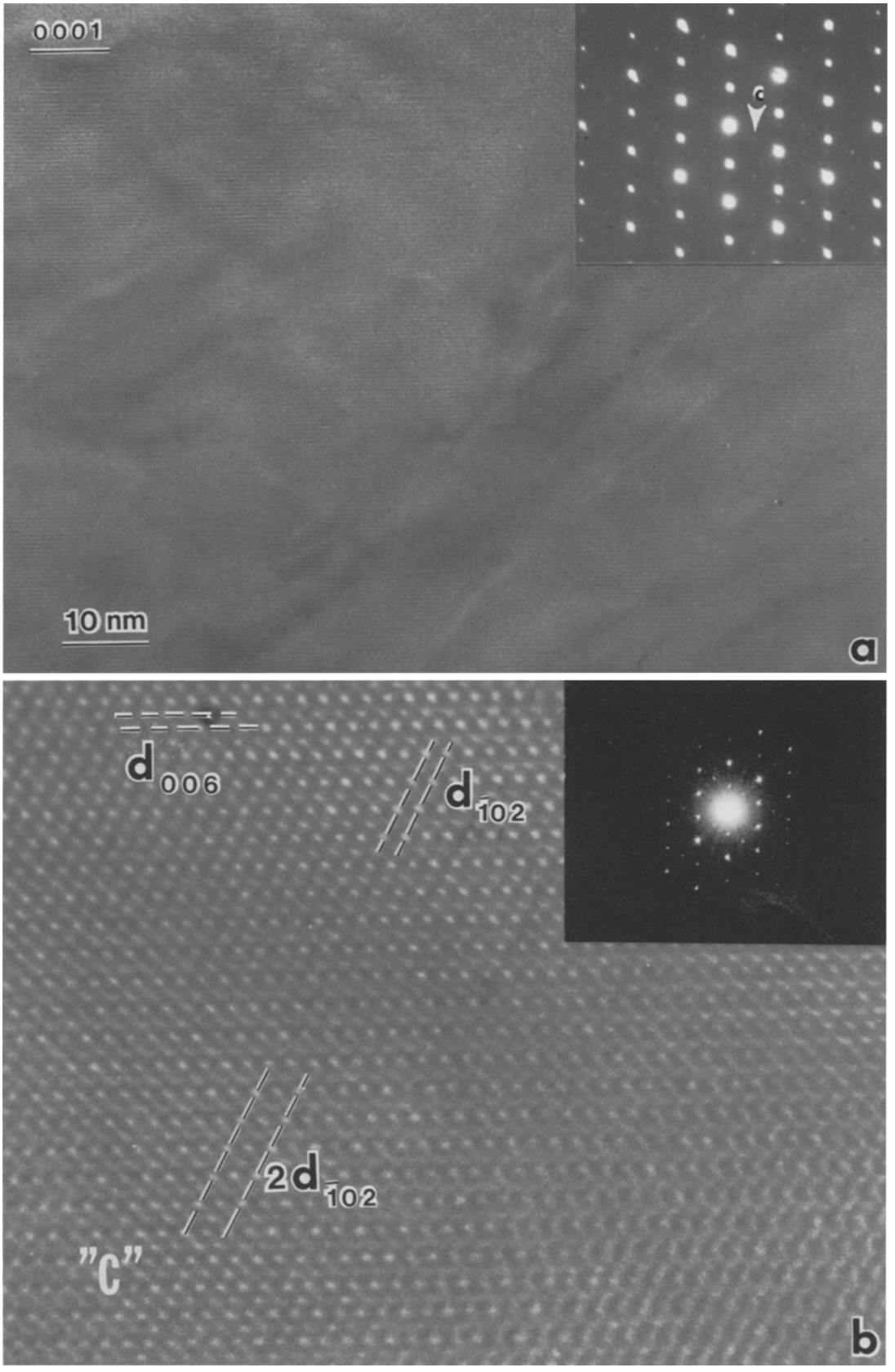

Fig. 5. **a** Low magnification, high resolution image along [11$\bar{2}$0] with "c" domains weakly visible. **b** High magnification image of a "c" domain (bottom) and adjacent ideal dolomite (top). Optical diffraction pattern of the "c" domain is inserted

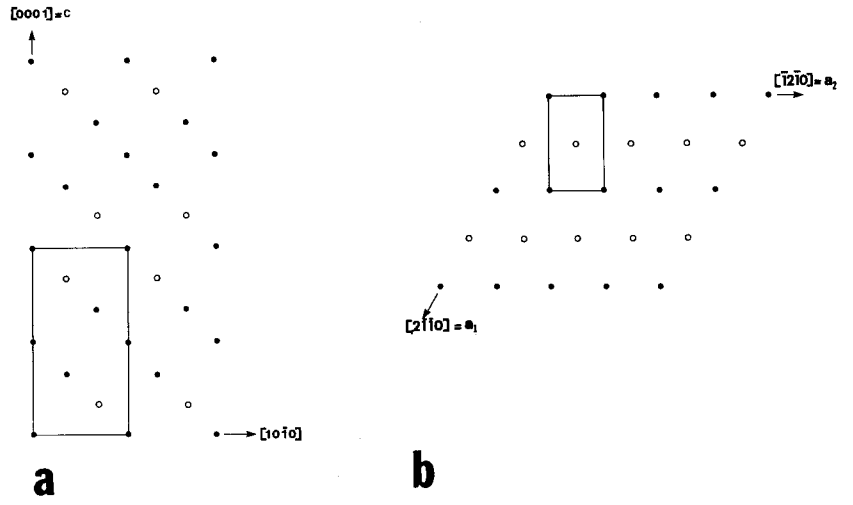

Fig. 6a, b. Models for cation distribution in superstructures of dolomite. Ca (●). Mg (○). **a** "d" type periodic intercalation of Ca in the dolomite type stacking disrupts the rhombohedral symmetry. **b** "c"-type basal plane with alternating rows of Ca and Mg which double the periodicity along a_1

is to substitute a Ca layer for every second Mg layer, resulting in

$$Ca^1-Mg^1-Ca^2-Ca^3-Ca^4-Mg^2-Ca^1\ldots$$

(Fig 6a). Such a cation arrangement is compatible with diffraction patterns like those in Figure 4d and yield a primitive hexagonal unit cell outlined in Figure 6a. The composition within this structure is $Ca_{0.67}Mg_{0.33}CO_3$. Any disorder in the stacking pattern produces diffuse streaks parallel to c^*. A similar diffraction pattern would result if two out of three Mg layers were substituted by Ca ($Ca_{0.83}Mg_{0.17}CO_3$). Note that the satellites are strongest about weaker dolomite "b" reflections which are due to the ordering of Mg and Ca. This supports the model that the presence of these satellites could be correlated with ordering of cations.

The "c" type reflections can be explained by ordering within the basal (0001) cation layers. If one (or more) of the originally pure Mg layers contains Ca as well as Mg, ordering can take place. For a $Mg_{0.5}Ca_{0.5}$ composition of the basal layer, alternating rows of Mg and Ca can be formed, thereby producing a doubling of one of the three a unit cell parameters. This destroys the threefold symmetry axis, and the structure becomes monoclinic ($P2/m$). The unit cell is outlined in Figure 6b. The composition of this superstructure (assuming that all Mg layers contain Mg and Ca) is $Ca_{0.75}Mg_{0.25}CO_3$. If the alternation of Mg and Ca in the basal plane is irregular or interrupted by non-conservative APB's, we expect streaking parallel to 110 in the diffraction pattern, as is observed in many dolomites with "c" reflections (Reeder 1981). Notice that such a structure has some similarities to that of huntite $Mg_{0.75}Ca_{0.25}CO_3$ (Graf and Bradley 1962), but the detailed cation distribution is different. Huntite appears to be rhombohedral, whereas c dolomite is not.

In very thin areas, we have noticed the absence of any "d" type domains on the high resolution images (Fig. 4a). This supports an ordering model for these domains. It is a common feature in ordered alloys that for very thin areas (3–10 nm) only the matrix is revealed; the intensity scattered into the superstructure reflections is too weak to compete with the strong basic (dolomite) reflections (see e.g., Van Tendeloo and Amelinckx 1981).

These two independent ordering phenomena (within the basal plane and between successive basal planes) can be easily combined to explain all observed diffraction patterns. Suppose that every third Mg layer is substituted by a mixed Mg–Ca layer instead of a pure Ca layer; this will still create a primitive hexagonal stacking along (0001) and introduce "d" type reflections. If this mixed layer is not ordered, no extra reflections will result. However, if ordering occurs within this layer (Fig. 6b), weak "c" type ordering reflections will be observed in the diffraction pattern. This explains why "c" type reflections can occur with or without "d" reflections being present.

Note that these models are based mainly on optical diffraction patterns of high resolution micrographs and analogy to superstructures observed in metal alloys. Whereas cation ordering is an obvious explanation for the observed structures, we are uncertain if and how the arrangement of anion groups may also contribute to the complexities in the diffraction patterns (Gunderson and Wenk 1981; Wenk et al. 1983). Because of the small size of the ordered domains this can probably only be determined by more high resolution microscopy, through focus series and quantitative contrast calculations, which are in progress.

6. Disordering Experiments

Irradiation of carbonates by electrons can produce decomposition into oxides, as documented by high resolution electron microscopy (Cater and Buseck 1985). In our experiments, we observed cation disordering. Cation disorder in dolomite has been the subject of several investigations, most notably by Goldsmith and Heard (1961), Reeder and Nakajima (1982), and Reeder and Wenk (1983). These studies document a second order transformation with a critical temperature of 1,100–1,150° C. Reordering upon cooling is very rapid, and it has never been possible to quench dolomite with an ordering parameter of less than 0.8. Microstructural observations of Reeder and Nakajima (1982) suggest that disorder at this temperature only involves cations and leaves anion groups largely ordered in contrast to $NaNO_3$.

When Lost Burro dolomite was studied in the ARM at 100 kV under a condensed beam, we noted that "c" type reflections disappeared after a few seconds (Fig. 7a), indicating disorder within the layers. Further exposure to the electron beam reduced the intensity of "b" reflections (Fig. 7b), which vanished completely after about 8 min

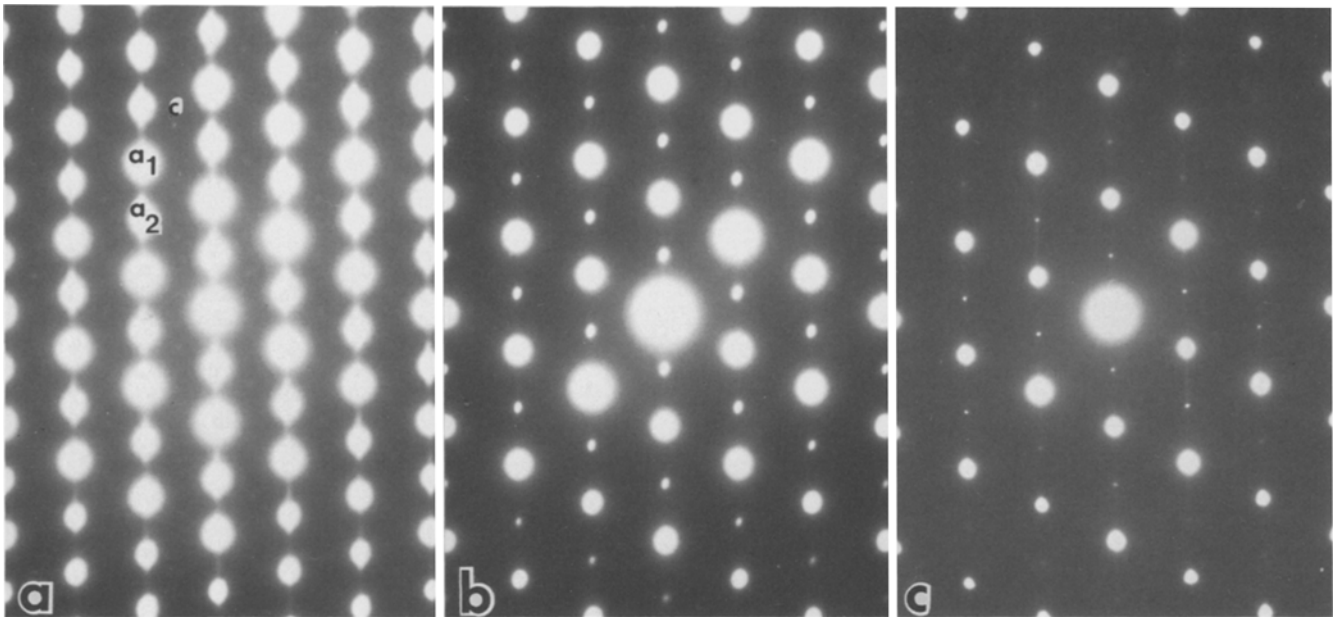

Fig. 7a–c. [11$\bar{2}$0] Diffraction patterns illustrating progressive disordering during in situ electron radiation in JEM ARM 1000. **a** 5 s; **b** 30 s; **c** 8 min

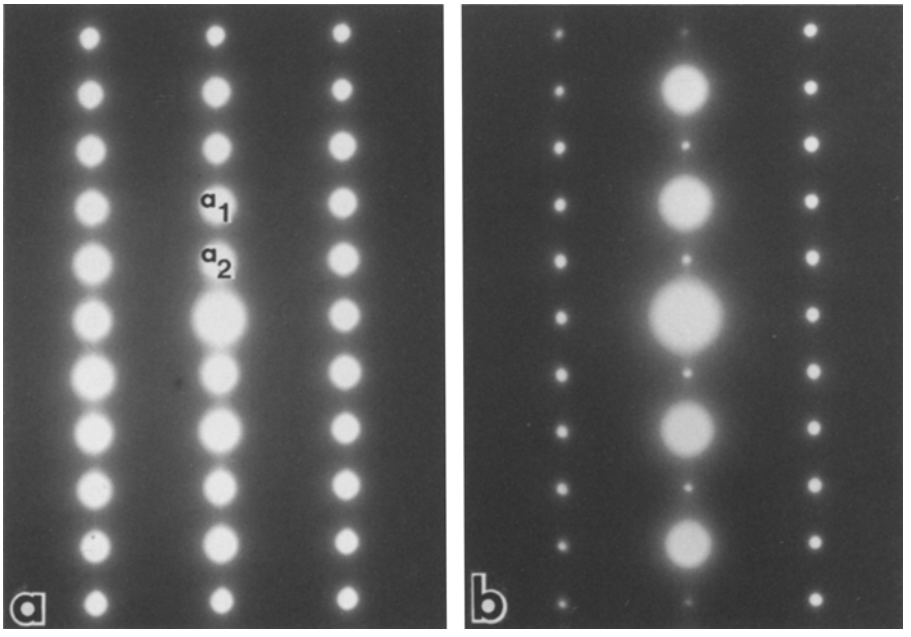

Fig. 8a, b. Diffraction patterns after electron irradiation. **a** Exactly along [10$\bar{1}$0]; **b** after tilting 5° around [0001]

(Fig. 7c). This pattern could be due to disordering of Ca and Mg or due to both anion and cation disorder. Only "a_1", "a_2" and "b" reflections remain, but tilting off the zone axis [100] eliminated "b" reflections (Fig. 8b), indicating that those present in Figure 8a were due to multiple diffraction. The "a_2" reflections remain strong and sharp, suggesting that CO_3 groups are still fully ordered and, in contrast to Cater and Buseck (1985), we did not observe any decomposition. These experiments were, of course, far from equilibrium conditions, but observations in alkali halides and metal alloys (Hobbs 1976; Banerjee et al. 1984) nevertheless suggest that disorder produced by radiation and thermal disorder can proceed by similar mechanisms.

If this applies also to carbonates, then it would indicate that in dolomite CO_3 groups are still ordered at 1,150° C when cation disorder occurs, confirming observations by Reeder and Nakajima (1982). Disorder occurs first within basal layers and then includes diffusion between adjacent layers, ultimately producing a calcite type structure.

Acknowledgements. We acknowledge support by the Office of Basic Energy Sciences, Contract DE-AC03-76SF00098, by NSF grants EAR 78 23848 and EAR 83 05865, and by a grant from the American Chemical Society PRF 13615-AC2. Professor D. Zenger kindly provided some of the specimens used in this study. Valuable discussions and comments by D.J. Barber, E.D. Cater and D. Veblen improved the manuscript and are appreciated.

References

Banerjee S, Urban K, Wilkens M (1984) Order-disorder transformation in Ni_4Mo under electron irradiation in a high voltage electron microscope. Acta Metall 32:299–311

Cater ED, Buseck PR (1985) Mechanism of decomposition of dolomite, $Ca_{.5}Mg_{.5}CO_3$ in the electron microscope. Ultramicroscopy (in press)

Goldsmith JR, Graf DL (1958) Relation between lattice constants and composition of the Ca–Mg carbonates. Am Mineral 43:84–101

Goldsmith JR, Heard HC (1961) Subsolidus phase relations in the system $CaCO_3-MgCO_3$. J Geol 69:45–74

Graf DL, Bradley WF (1962) The crystal structure of huntite, $Mg_3Ca(CO_3)_4$. Acta Crystallogr 15:238–242

Gunderson SH, Wenk HR (1981) Heterogeneous microstructures in oolitic carbonates. Am Mineral 66:789–800

Hobbs L (1976) Radiation effects in the electron microscopy of beam sensitive inorganic solids. In: Venables JA (ed) Developments in Electron Microscopy and Analysis. Academic Press New York, pp 287–292

O'Keefe MA, Barber DJ (1984) Interpretation of HREM images of dolomite. Inst Phys Conf Ser No 68: Chapter 5, pp 177–180

Paul GL, Pryor AW (1971) The study of sodium nitrate by neutron diffraction. Acta Crystallogr B27:2700–2702

Reeder RJ (1981) Electron optical investigation of sedimentary dolomites. Contrib Mineral Petrol 76:148–157

Reeder RJ, Nakajima Y (1982) The nature of ordering and ordering defects in dolomite. Phys Chem Minerals 8:29–35

Reeder RJ, Wenk HR (1979) Microstructures in low temperature dolomites. Geophys Res Lett 6:77–80

Reeder RJ, Wenk HR (1983) Structure refinements of some thermally disordered dolomites. Am Mineral 68:769–776

Schryvers D, Van Landuyt J, Ven Tendeloo G, Amelinckx S (1983) Electron microscopy study of two new long period structures in Pt_xTi alloys ($3<x<8$). Phys Status Solidi (a) 76:575–593

Sinclair R, Gronsky R, Thomas G (1976) Optical diffraction from lattice images of alloys. Acta Metall 24:789–796

Tanji T, Hashimoto H (1978) Optical selected area diffraction patterns of high resolution electron microscope images for crystal analysis. Acta Crystallogr A34:453–459

Van Tendeloo G, Amelinckx S (1981) Electron diffraction and high resolution electron microscopy study of ordering in gold-manganese systems (I and II). Phys Status Solidi (a) 65:73–86 and 65:431–446

Van Tendeloo G, Van Landuyt J (1983) The use of optical diffraction in materials science. J Microsc Spectrosc Electronique 8:461–480

Van Tendeloo G, Van Landuyt J, Delavignette P, Amelinckx S (1974) Compositional changes associated with periodic antiphase boundaries in the initial stages of ordering in Ni_3Mo. Phys Status Solidi (a) 25:697–707

Wenk HR, Barber DJ, Reeder RJ (1983) Microstructures in Carbonates. In: Reeder RJ (ed) Carbonates: Mineralogy and Chemistry: Rev in Mineralogy 11:pp 301–367, Min Soc Am

Wenk HR, Zenger DH (1983) Sequential basal faults in Devonian dolomite, Nopah Range, Death Valley area, California. Science 222:502–504

Zenger DH (1983) Burial dolomitization in the Lost Burro Formation (Devonian), east-central California and the significance of late diagenetic dolomitization. Geology 11:519–522

Received August 27, 1984